

## Structural and Morphological Characterization of MEH-PPV/Ag Composite

Suha Ahmad Jawad<sup>1a</sup> and Mustafa Mohammed Ali Hussein<sup>1b\*</sup>

<sup>1</sup>*Department of Physics, College of Science, University of Baghdad, Baghdad, Iraq*

<sup>a</sup>E-mail: [soha.ahmed1604a@sc.uobaghdad.edu.iq](mailto:soha.ahmed1604a@sc.uobaghdad.edu.iq)

<sup>b\*</sup>Corresponding author: [mustafa.hussein@sc.uobaghdad.edu.iq](mailto:mustafa.hussein@sc.uobaghdad.edu.iq)

### Abstract

In this study, spin coating was used to prepare thin films of poly (2-methoxy-5-(2-ethylhexyloxy)-1, 4-phenylene vinylene) and silver (MEH-PPV/Ag) in this study. The physical characteristics of MEH-PPV/Ag thin films with various weight ratios (0.01, 0.02, 0.03, and 0.04%) were investigated by Fourier-transform infrared spectroscopy (FTIR), field emission scanning electron microscopy (FE-SEM), atomic force microscopy (AFM), X-ray diffraction analysis (XRD), and thermal testing. FTIR analysis showed that there were occurrences of the polymer's predicted chemical bonds. AFM tests show that when different amounts of silver are added to a polymer matrix, the film's surface roughness (root mean square) goes up from an average of 83.51 to 511.3 nm. FE-SEM analysis showed that a pure sample of the polymer formed evenly. However, when different amounts of Ag were added, clear balls or circles formed, showing the energy of mixing between the MEH-PPV and Ag. As silver addition transformed the polymer from amorphous to polycrystalline, XRD analysis revealed both phases. In tests comparing pure MEH-PPV to MEH-PPV/Ag, the polymer containing silver showed higher thermal conductivity.

### Article Info.

#### Keywords:

*MEH-PPV/Ag Thin Films, FTIR, FE-SEM, XRD, Thermal Conductivity.*

#### Article history:

*Received: May 15, 2023*

*Revised: Sep. 16, 2023*

*Accepted: Oct. 15, 2023*

*Published: Mar. 01, 2024*

### 1. Introduction

Poly (phenylenevinylene) (PPV) is the only polymer of its type that can be treated into a highly ordered crystalline thin film [1-9], and its conjugated nature has received a lot of attention since it becomes electrically conductive upon doping. Using conducting polymer materials as an active medium has led to the development of several optoelectronic devices, including field effect transistors, light-emitting diodes (LED), and photo-diodes (bulk heterojunction) [10-19].

Among these significant polymer classes is poly(2-methox-5(2'-ethylhexyloxy)-1,4-phenylene vinylene (MEH-PPV), which has received a great deal of attention since it was the first PPV to be soluble in commonly used organic solvents [20-29]. It has been successfully used as a highly efficient light-emitting material in electroluminescence devices. Due to its semiconducting characteristics, MEH-PPV has been the subject of much research. Thin films may be made with PPV derivatives like MEH-PPV. Thin films can be used to create organic light-emitting diodes (OLED) and solar cell devices [30-39]. Organic polymers with molecular orbitals distributed over the whole polymer chain are called "conjugated polymers." These orbitals are represented in chemical structural formulas by a series of linked figures that switch between single and double carbon bonds, Fig.1.

Since the finding of high conductance in doped polyacetylene [40], several researchers have focused their attention on these polymers. The Nobel Prize in Chemistry was given to Alan J. Heeger, Alan G. MacDiarmid and Hideki Shirakawa in 2000 for their work on this finding [41]. The fascination with conjugated polymers stems from their exceptional mix of characteristics [42-46]. The polymer found in light-emitting polymers conducts electricity when subjected to a voltage [46, 47]. Others researchers in 2022 focused on manufacturing certain thin films used gas detectors to



improve their quality. They also produced a thin film of MEH-PPV/ $\text{FeCl}_3$  and conducted studies on it, resulting in fairly comparable results to those that others had obtained [48]. The aim of this work is to study the structural and morphological characterization of MEH-PPV composites doped with different ratios of silver through different tests.

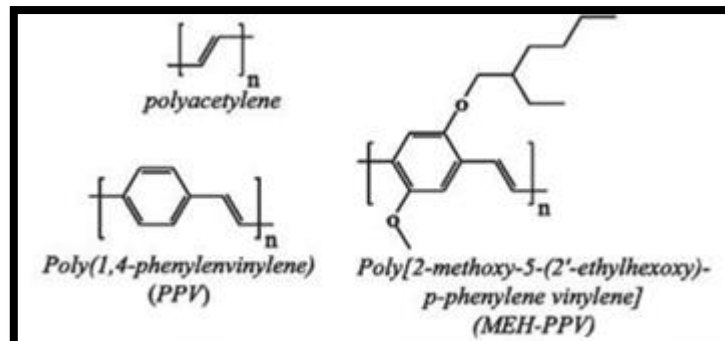


Figure 1: Structure formula of some  $\pi$ -conjugated polymers [48].

## 2. Experimental Work

### 2.1. Materials

The orange powder of MEH-PPV with 99.99% purity that is used in this work was purchased from American Dye Source Inc. Canada. The silver metal powder with a purity of 99.99% was purchased from HIMEDIA, India Laboratories Pvt. Ltd. Also, the solvent toluene with a purity of 99.7% was purchased from Thermo Scientific Chemicals, France.

### 2.2. Preparation of Specimens and Thickness Measurement

To produce MEH-PPV solution, 210 mg of its powder was dissolved in 75 ml of toluene solvent, and the solution was stirred with a magnetic stirrer for at least 5 hours. Adding silver micro-particle powder with various ratio concentrations (0.01, 0.02, 0.03, and 0.04 %) to the solution and using a magnetic stirrer, the mixing of MEH-PPV/Ag was accomplished. Then each concentration was put in a glass tube and left for 4hrs at room temperature, so homogenous solutions of MEH-PPV/Ag were produced. After that, thin films were uniformly distributed on (2.5  $\times$  2.5) cm glass slides, which were cleaned with a solution of distilled water and alcohol, and dried in an oven, using the spin coating technique. The desired amount of the solution was put onto the glass slides using a micropipette, the device was set to rotate at a rate of one thousand revolutions per minute (rpm). Fourier-transform infrared spectroscopy (FTIR), field emission scanning electron microscopy (FE-SEM), atomic force microscopy (AFM), X-ray diffraction analysis (XRD) techniques were employed to characterize the films. Thermal conductivity of MEH-PPV and MEH-PPV/Ag also was measured.

The thickness of the films was measured using AFM. The thickness of the samples was determined by calculating the height difference between the material-coated and uncoated area, and averaging the two values. The sample's thickness was 453.6 nm, as shown in Fig. 2.

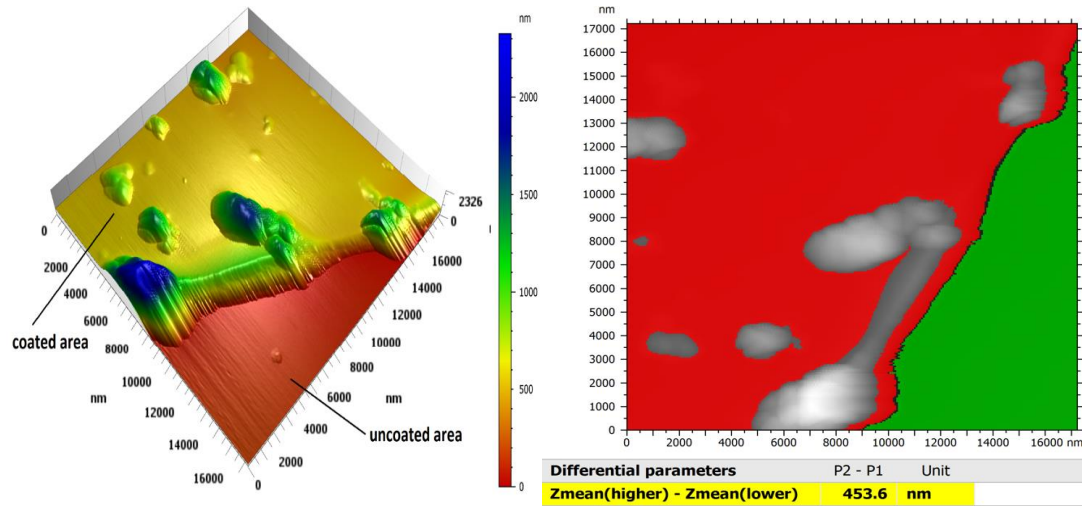
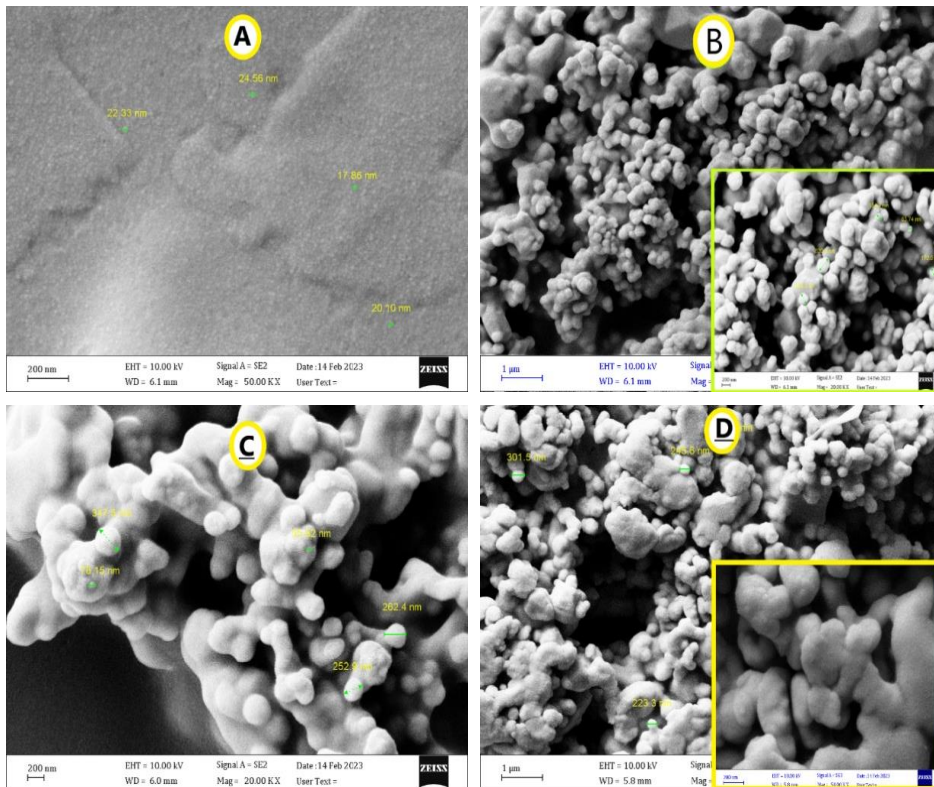


Figure 2: AFM scan images for specimen thickness measurement.

### 3. Results and Discussion

#### 3.1. Field-Emission Scanning Electron Microscopy (FE-SEM)

The growth of the MEH-PPV pure film is clearly uniform, as shown in Fig. 3 for MEH-PPV and MEH-PPV/Ag with different weight ratios. FE-SEM studies show that there is a network of microscopic fractures with different lengths and directions. Under thermal pressure, oxide-scale cracking is what causes these. This occurs as a result of cyclic transitional thermal gradients caused by repeated heating and cooling of the surface. When doping material (Ag) is added to MEH-PPV at various weight percentages (0.01, 0.02, 0.03, and 0.04%), the formation of prominent or clear circles indicates adsorption [9]. The adsorption increases as the number of dopants increases. At a ratio of 0.03% of MEH-PPV/Ag, the sample exhibits the highest adsorption energy.



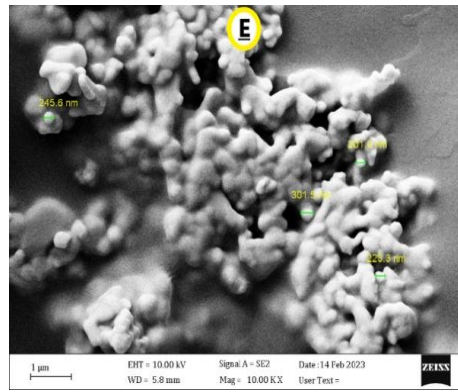


Figure 3: FE-SEM images of: A- pure MEH-PPV, B- MEH-PPV/Ag (0.01%), C- MEH-PPV/Ag (0.02%), D- MEH-PPV/Ag (0.03%), and E- MEH-PPV/Ag (0.04%).

### 3.2. X-Ray Diffraction (XRD)

The X-ray diffraction pattern was used to look at the pure MEH-PPV-coated glass samples and the silver-doped samples with varying amounts (0.02 and 0.04%) to find out whether the material was crystalline or not. The test revealed that no crystalline peaks appeared on the films deposited on the glass substrates of the pure MEH-PPV material. This result confirms that the polymer MEH-PPV has an amorphous nature. While the XRD pattern has shown numerous peaks or reflections when MEH-PPV is doped with silver at varying concentrations, peaks appear at the following angles:  $38.22^\circ$ ,  $44.38^\circ$ ,  $64.6^\circ$ , and  $77.70^\circ$ , corresponding to (111), (200), (220), and (311) groups of lattice levels, respectively, as shown in Fig. 4 and Table 1, which can be classified as a type of face cube center (FCC), which is the structure of silver nanoparticles.

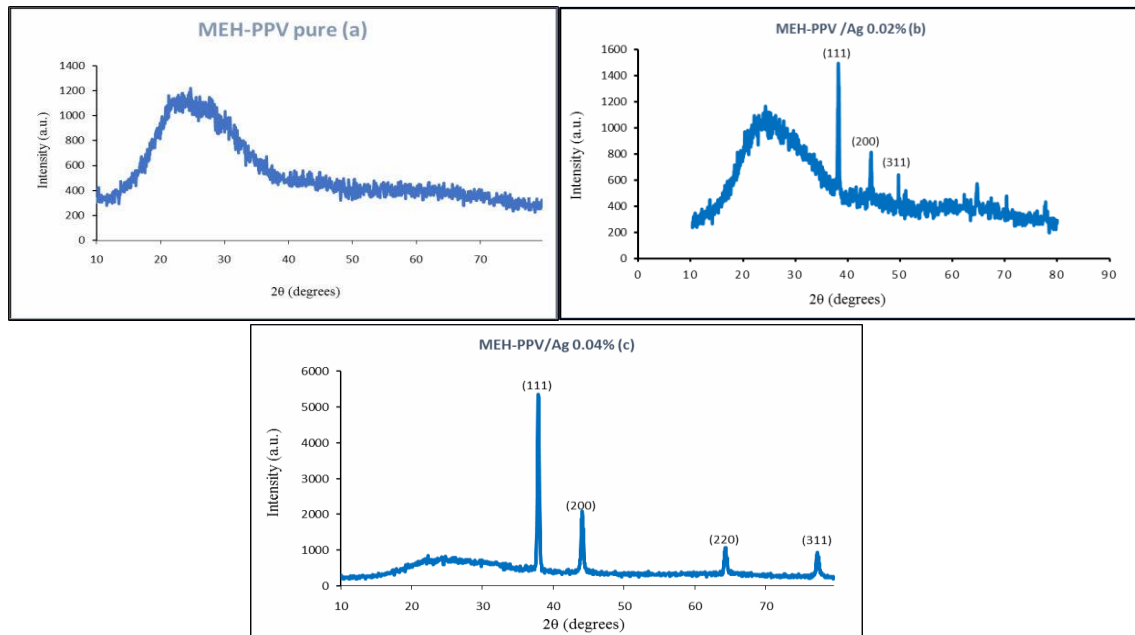


Figure 4: XRD patterns of (a) pure MEH-PPV, (b) MEH-PPV/Ag (0.02%), and (c) MEH-PPV/Ag (0.04%).

Table 1: X-ray diffraction peak list of silver nanoparticles.

2θ (Degree)	Intensity (a.u.)	FWHM (Degree)	d-Spacing (Å)
38.22	4948.38	0.2460	2.35
44.38	1498.07	0.295	2.04
64.6	720.81	0.344	1.442
77.70	85.19	0.24	1.22

### 3.3. Atomic Force Microscope Analysis (AFM)

The AFM was used to evaluate the morphology and surface roughness of MEH-PPV and MEH-PPV/Ag films on a substrate surface. Taking phase pictures with an AFM in tapping mode can also show material details about the surface of a film. This is because a change in dispersive power in a non-elastic tip-sample contact makes a solid material show a positive phase transition compared to a soft material. The surface structure and shapes of pure MEH-PPV and MEH-PPV/Ag at different concentrations are shown in the 2D and 3D images that follow. Fig. 5 and Table 2 show that when different amounts of silver are added to a polymer matrix, the film's surface roughness (root mean square) goes up from an average of 83.51 to 511.3 nm.

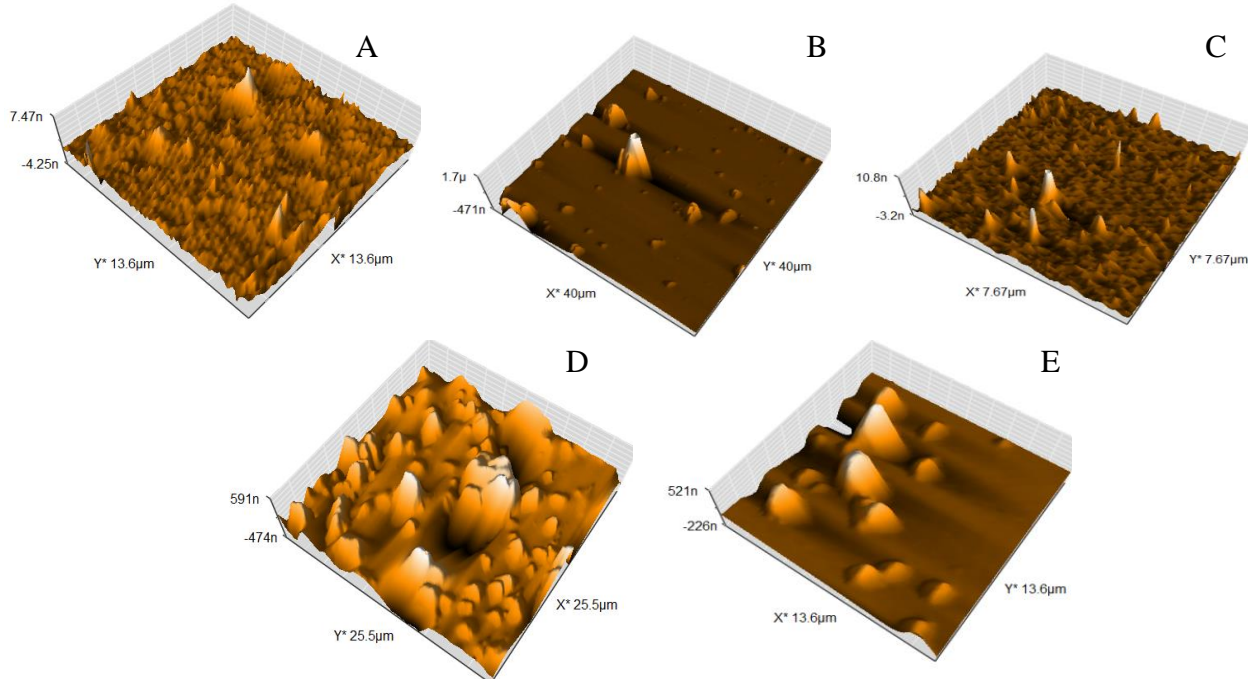


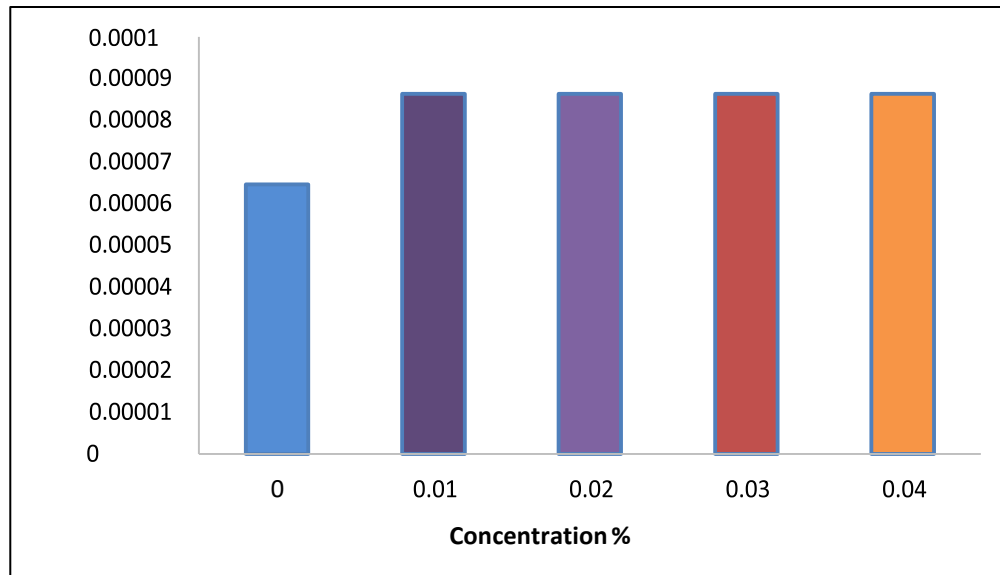
Figure 5: 2D and 3D AFM images of: (A) pure MEH-PPV, (B) MEH-PPV/Ag (0.01%), (C) MEH-PPV/Ag (0.02%), (D) MEH-PPV/Ag (0.03%), and (E) MEH-PPV/Ag (0.04%).

Table 2: Values for mean roughness, particle height rate, mean diameter, and root mean square of MEH-PPV/Ag at different ratios of Ag.

Sample	Rq (nm)	Ra (nm)	Z max (nm)	Mean diameter (nm)
MEH-PPV/Ag	Root mean square	Average roughness		
Pure (0%)	83.51	38.39	350.5	68.03
0.01%	24.18	97.60	7408	401.7
0.02%	276.4	162.3	5615	771.2
0.03%	376.2	276.9	3646	304.2
0.04%	511.3	374.7	2729	157.1

### 3.4. Thermal Conductivity

Thermal conductivity attempts to measure an object's capacity to conduct heat. The objective of the thermal conductivity test is to quantify the polymer's thermal conductivity and track its evolution in response to varying concentrations of silver doping. The graph below represents the increase in thermal conductivity of the polymer after the addition of silver. The conductivity of the polymer increased when the silver was added. Fig. 6 demonstrates that the conductivity of the polymer was observed to rise as Ag was added to the MEH-PPV polymer.



**Figure 6:** Thermal conductivity of the pure polymer and MEH-PPV/Ag at different ratios of Ag (0.01, 0.02, 0.03, and 0.04 %).

### 3.5. Fourier Transform Infrared Spectroscopy (FTIR)

FTIR spectroscopy looks at multicomponent functional groups to help us understand how reactions work and to find out what the substance phase is made of in all the different types of bonds that are present in the samples. Fig. 7 demonstrates FTIR spectra for pure MEH-PPV and MEH-PPV/Ag (0.01, 0.02, 0.03 and 0.04 wt %). As shown in Table 3, the spectra reveal separated bands. Peaks at  $3433\text{ cm}^{-1}$  in pure MEH-PPV correspond to N-H stretching vibration. At  $3055.3\text{ cm}^{-1}$ , peaks correspond to C-H: sp<sup>2</sup> C-H (stretching mode). O-H stretching mode corresponds to peaks at  $2954\text{ cm}^{-1}$  (carboxylic acid). The peak at  $2858\text{ cm}^{-1}$  corresponds to carbon-hydrogen (stretching mode). C=O stretching mode corresponds to peaks at  $1643\text{ cm}^{-1}$  (conjugation of an aldehyde with two aromatic rings). These results support M. Ibrahim and others' position [47]. C=C aromatic ring corresponds to the peaks at  $1577\text{ cm}^{-1}$ . According to J. S. Shankar et al. [49], peaks at  $1411\text{ cm}^{-1}$  correspond to C-O-H (bending mode) and  $975.98\text{ cm}^{-1}$  correspond to vinyl oxygen expansion and alkyl oxygen expansion, respectively. Regarding the addition of Ag at various weight ratios, there was a great similarity between the peaks that appeared in pure material and a new peak at  $475\text{ cm}^{-1}$  correspond to Ag that did not appear in the pure state.

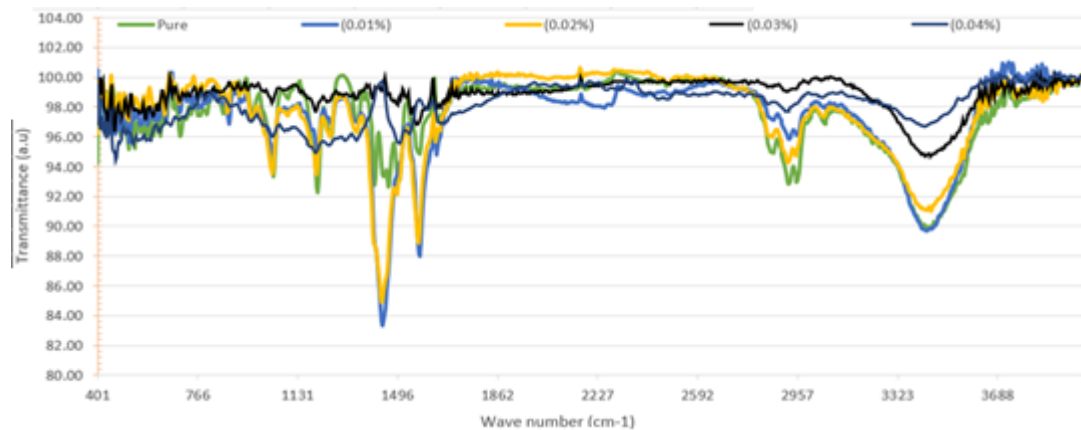


**Figure 7:** FTIR spectra for of the pure polymer and MEH-PPV/Ag at different ratios of Ag (0.01, 0.02, 0.03, and 0.04 %).

**Table 3: Active groups affiliate with FTIR peaks for all samples.**

Bond type	Wave Number (cm <sup>-1</sup> )				
	Pure	0.01%	0.02%	0.03%	0.04%
N-H	3433	3448	3429	3429	3425
C-H:sp <sup>2</sup> C-H	3055	3055	3055	3053	3051
O-H	2954,2924	3236,2870	2924,2858	2924	2924
C-H	2858	3236	2858	2854	2850
C=O	1643	1639	1639	1643	1658
C=C	1577	1577	1577+1500	1573	1612+1508
C-O-H	1411	1350	1350	1411	1350
C-O	1203+1041	1253+1203	1203	1203	1249
=C-H Out-of-plane bending mode	968+702	702	968+879	794+702	964+844

#### 4. Conclusions

Thin films of MEH-PPV and MEH-PPV/Ag with varying weight ratios were effectively produced using spin coating and drop casting processes. The FTIR spectra of the samples exhibited the known MEH-PPV peaks. When Ag was introduced at various weight ratios, a new peak of 474 cm<sup>-1</sup> developed, and this peak belonged to Ag, indicating that Ag is not chemically reacted but rather creates a composite. AFM tests show that when different amounts of silver are added to a polymer matrix, the film's surface roughness (root mean square) goes up from an average of 83.51 to 511.3 nm. The FE-SEM analysis revealed that pure MEH-PPV films had a uniform and regular appearance; however, when Ag was added at various weight ratios, conspicuous circles developed, suggesting the existence of adsorption energy, with the greatest adsorption energy created at the MEH-PPV/Ag interface (0.03 %). Not only was the polymer's thermal conductivity tested, but it was also proven that adding silver to the mixture made it more conductive.

#### Acknowledgment

The authors would like to express their sincere gratitude to Dr. Omar Adnan, who somewhat helped us in the work on this article.

#### Conflict of Interest

Authors declare that they have no conflict of interest.

#### References

1. D. M. Bobrowska, K. Gdula, J. Breczko, A. Basa, K. H. Markiewicz, and K. Winkler, *J. Nanopart. Res.* **24**, 222 (2022).
2. J. Banerjee and K. Dutta, *Chem. Pap.* **75**, 5139 (2021).
3. C. A. Young, A. Hammack, H. J. Lee, H. Jia, T. Yu, M. D. Marquez, A. C. Jamison, B. E. Gnade, and T. R. Lee, *ACS Omega*, **4**, 22332 (2019).
4. J. R. Reynolds and T. A. Skotheim, *Handbook of Conducting Polymers: Theory, Synthesis, Properties, and Characterization. Conjugated Polymers* (New York, CRC Press, 2007).
5. T. Granier, E. L. Thomas, D. R. Gagnon, F. E. Karasz, and R. W. Lenz, *J. Poly. Sci. P. B: Poly. Phys.* **24**, 2793 (1986).
6. J. H. Burroughes, D. D. Bradley, A. Brown, R. Marks, K. Mackay, R. H. Friend, P. L. Burns, and A. B. Holmes, *Nature* **347**, 539 (1990).

7. D. Moses, *Appl. Phys. Lett.* **60**, 3215 (1992).
8. J. Li, N. Sun, Z.-X. Guo, C. Li, Y. Li, L. Dai, D. Zhu, D. Sun, Y. Cao, and L. Fan, *J. Phys. Chem. B* **106**, 11509 (2002).
9. N. S. Sariciftci, D. Braun, C. Zhang, V. Srdanov, A. J. Heeger, G. Stucky, and F. Wudl, *Appl. Phys. Lett.* **62**, 585 (1993).
10. Z. L. Zhang, X. Y. Jiang, W. Q. Zhu, X. Y. Zheng, Y. Z. Wu, and S. H. Xu, *Synth. Met.* **137**, 1141 (2003).
11. A. R. Murad, A. Iraqi, S. B. Aziz, S. N. Abdullah, and M. A. Brza, *Polymers* **12**, 2627 (2020).
12. D. Khokhar, S. Jadoun, R. Arif, and S. Jabin, *Poly. Plas. Tech. Mat.* **60**, 465 (2021).
13. D. Abbaszadeh, A. Kunz, N. B. Kotadiya, A. Mondal, D. Andrienko, J. J. Michels, G.-J. A. Wetzelaer, and P. W. Blom, *Chem. Mat.* **31**, 6380 (2019).
14. N. B. Kotadiya, A. Mondal, P. W. Blom, D. Andrienko, and G.-J. A. Wetzelaer, *Nat. Mat.* **18**, 1182 (2019).
15. N. B. Kotadiya, P. W. Blom, and G.-J. A. Wetzelaer, *Nat. Photon.* **13**, 765 (2019).
16. Y. Li, M. Kovačić, J. Westphalen, S. Oswald, Z. Ma, C. Hänisch, P.-A. Will, L. Jiang, M. Junghaehnel, R. Scholz, S. Lenk, and S. Reineke, *Nat. Commun.* **10**, 2972 (2019).
17. M. Kettner, Z. Mi, D. Kälblein, J. Brill, P. W. Blom, and R. T. Weitz, *Adv. Elect. Mat.* **5**, 1900295 (2019).
18. L. Q. Flagg, C. G. Bischak, J. W. Onorato, R. B. Rashid, C. K. Luscombe, and D. S. Ginger, *J. American Chem. Soci.* **141**, 4345 (2019).
19. K. Lieberth, A. Pavlou, D. Harig, P. W. Blom, P. Gkoupidenis, and F. Torricelli, *Adv. Mat. Tech.* **8**, 2201697 (2023).
20. B. Briou, B. Améduri, and B. Boutevin, *Chem. Soci. Rev.* **50**, 11055 (2021).
21. H. Xia, C. Hu, T. Chen, D. Hu, M. Zhang, and K. Xie, *Polymers* **11**, 443 (2019).
22. A. M. Díez-Pascual, *Polymers* **14**, 1979 (2022).
23. M. Naffakh, *Polymers* **13**, 2947 (2021).
24. M. Naffakh, P. Rica, C. Moya-Lopez, J. A. Castro-Osma, C. Alonso-Moreno, and D. A. Moreno, *Polymers* **13**, 2214 (2021).
25. D. Chen, S. K. Tiwari, Z. Ma, J. Wen, S. Liu, J. Li, F. Wei, K. Thummavichai, Z. Yang, and Y. Zhu, *Polymers* **12**, 2342 (2020).
26. J. A. Luceño-Sánchez, A. M. Díez-Pascual, and R. Peña Capilla, *Int. J. Molec. Sci.* **20**, 976 (2019).
27. B. A. Al-Asbahi, S. M. Qaid, M. H. Hj. Jumali, M. S. Alsalhi, and A. S. Aldwayyan, *J. Appl. Poly. Sci.* **136**, 47845 (2019).
28. S. Al-Bati, M. H. Hj. Jumali, B. A. Al-Asbahi, K. Ibtehaj, C. C. Yap, S. M. Qaid, H. M. Ghaithan, and W. Farooq, *Polymers* **12**, 2154 (2020).
29. B. A. Al-Asbahi, M. H. Hj. Jumali, M. Alsalhi, S. M. Qaid, A. Fatehmulla, W. M. Mujamammi, and H. M. Ghaithan, *Polymers* **13**, 611 (2021).
30. C. Galey and H. Park, *AIP Advances* **9**, 105010 (2019).
31. L. Mao, J. Xie, H. Wu, and Y. Liu, *Polymers* **12**, 2093 (2020).
32. A. Islam, S. H. U. Shah, Z. Haider, M. Imran, A. Amin, S. K. Haider, and M.-D. Li, *Micromachines* **14**, 1171 (2023).
33. M. Riede, D. Spoltore, and K. Leo, *Adv. En. Mat.* **11**, 2002653 (2021).
34. J. Song, H. Lee, E. G. Jeong, K. C. Choi, and S. Yoo, *Adv. Mat.* **32**, 1907539 (2020).
35. Y. Cui, H. Yao, J. Zhang, T. Zhang, Y. Wang, L. Hong, K. Xian, B. Xu, S. Zhang, and J. Peng, *Nat. Communic.* **10**, 2515 (2019).

36. T. Li, Z. Chen, Y. Wang, J. Tu, X. Deng, Q. Li, and Z. Li, ACS Appl. Mat. Inter. **12**, 3301 (2019).
37. F. Zhao, J. Zhou, D. He, C. Wang, and Y. Lin, J. Mat. Chem. C **9**, 15395 (2021).
38. H. Pham, En. Environ. Sci. **12**, 1177 (2019).
39. J. Li, N. Wang, Y. Wang, Z. Liang, Y. Peng, C. Yang, X. Bao, and Y. Xia, Sol. En. **196**, 168 (2020).
40. S. Meftah, M. Benhaliliba, M. Kaleli, C. Benouis, C. Yavru, and A. Bayram, J. Elect. Mat. **50**, 2287 (2021).
41. G. Sharma, S. Kattayat, S. F. Naqvi, S. Hashmi, and P. Alvi, Mat. Today Proceed. **42**, 1678 (2021).
42. S. M. Qaid, B. A. Al-Asbahi, H. M. Ghaithan, and A. S. Aldwayyan, Coatings **11**, 154 (2021).
43. S. Erdönmez, Y. Karabul, M. Kılıç, Z. Güven Özdemir, and K. Esmer, Poly. Comp. **42**, 1347 (2021).
44. R. Ilyas, S. Sapuan, M. Asyraf, D. Dayana, J. Amelia, M. Rani, M. N. F. Norrrahim, N. Nurazzi, H. Aisyah, and S. Sharma, Polymers **13**, 1701 (2021).
45. J. S. Chohan, N. Mittal, R. Kumar, S. Singh, S. Sharma, S. P. Dwivedi, A. Saxena, S. Chattopadhyaya, R. A. Ilyas, and C. H. Le, Polymers **13**, 1702 (2021).
46. S. I. Sharhan and I. M. Ibrahim, Iraqi J. Sci. **60**, 754 (2019).
47. S. Ashok Kumar, J. S. Shankar, and B. K. Periyasamy, Semicond. Sci. Tech. **37**, 045015 (2022).
48. N. M. Jabbar and M. M.-A. Hussein, Iraqi J. Phys. **20**, 109 (2022).
49. J. S. Shankar, S. Ashok Kumar, B. K. Periyasamy, and S. K. Nayak, Poly. Plast. Tech. Mat. **58**, 148 (2019).

## الخصائص الهيكلية والتضاريسية لمركب MEH-PPV/Ag

سهى احمد جواد<sup>1</sup> ومصطفى محمد علي حسين<sup>1</sup>  
<sup>1</sup> قسم الفيزياء، كلية العلوم، جامعة بغداد، بغداد، العراق

### الخلاصة

في هذا البحث، تم استخدام تقنية الطلاء الدوراني لتحضير أغشية رقيقة من البولي (2-ميثوكسي-5-(2-إيثيلهكسيلوكسي) -1، -4-فينيلين فينيلين)/الفضة (MEH-PPV/Ag). تم دراسة الخصائص الفيزيائية للأغشية الرقيقة MEH-PPV/Ag ذات نسب وزن مختلفة (0.01، 0.02، 0.03، و0.04%) بواسطة التحليل الطيفي للأشعة تحت الحمراء لتحويل فورييه (FTIR)، المجهر الإلكتروني لمسح الانبعاث الميداني (FE-SEM)، الفحص المجهرية بالقوة الذرية (AFM)، وتحليل حيود الأشعة السينية (XRD)، والاختبار الحراري. أظهر تحليل FTIR وجود روابط كيميائية متوقعة للبوليمر. تظهر اختبارات AFM أنه عند إضافة كميات مختلفة من الفضة إلى مصفوفة بوليمر، فإن خشونة سطح الفيلم (جنر متوسط المربع) ترتفع من متوسط 83.51 إلى 511.3 نانومتر. كشف تحليل FE-SEM أنه بينما تشكلت عينة نقية من البوليمر بالتساوي، عند إضافة Ag بنسب وزن مختلفة، تطورت كرات أو دوائر مميزة وواضحة، مما يكشف عن طاقة الخلط بين MEH-PPV والفضة. عندما أدت إضافة الفضة إلى تحويل البوليمر من غير متبلور إلى متعدد البلورات، كشف تحليل XRD عن كلا المرحلتين. في الاختبارات التي تقارن MEH-PPV النقي مع MEH-PPV/Ag، أظهر البوليمر المحتوي على الفضة موصلية حرارية أعلى.

**الكلمات المفتاحية:** أغشية MEH-PPV/Ag الرقيقة، التحليل الطيفي للأشعة تحت الحمراء لتحويل فورييه، المجهر الإلكتروني لمسح الانبعاث الميداني، الفحص المجهرية بالقوة الذرية، تحليل حيود الأشعة السينية، التوصيلية الحرارية.